

Regioselective One-Step Synthesis and Topological Chirality of *trans-3, trans-3,trans-3* and *e,e,e* [60]Fullerene-Cyclotrimeratrylene Tris-adducts: Discussion on a Topological *meso*-Form

by Gwénaël Rapenne

Groupe d'Electronique Moléculaire, CEMES-CNRS UPR 8011, 29 rue Jeanne Marvig, F-31055 Toulouse Cedex 4

and Jeanne Crassous

Laboratoire de Stéréochimie et des Interactions Moléculaires, CNRS UMR 5532, Ecole Normale Supérieure de Lyon 46, Allée d'Italie, F-69364 Lyon Cedex 7

and Lourdes E. Echegoyen and Luis Echegoyen

Department of Chemistry, University of Miami, Coral Gables, FL 33124, USA

and Erica Flapan

Department of Mathematics, Pomona College, Claremont, CA 91711, USA

and François Diederich*

Laboratorium für Organische Chemie, ETH-Zentrum, Universitätstrasse 16, CH-8092 Zürich
(Fax: +41-1-632 11 09; e-mail: diederich@org.chem.ethz.ch)

In memoriam Prof. André Collet

The C_3 -symmetrical [60]fullerene-cyclotrimeratrylene (CTV) tris-adducts (\pm)-**1** (with a *trans-3,trans-3,trans-3* addition pattern) and (\pm)-**2** (with an *e,e,e* addition pattern) were prepared in 11 and 9% yield, respectively, by the regio- and diastereoselective tether-directed *Bingel* reaction of C_{60} with the tris-malonate-appended CTV derivative (\pm)-**3** (*Scheme*). This is the first example for tris-adduct formation by a one-step tether-directed *Bingel* addition. Interchromophoric interactions between the electron-rich CTV cap and the electron-attracting fullerene moiety have a profound effect on the electrochemical behavior of the C-sphere (*Fig. 4* and *Table 1*). The fullerene-centered first reduction potentials in compounds (\pm)-**1** and (\pm)-**2** are by 100 mV more negative than those of their corresponding tris[bis(ethoxycarbonyl)methano][60]fullerene analogs that lack the CTV cap. A particular interest in (\pm)-**1** and (\pm)-**2** arises from the topological chirality of these molecules. A complete topology study is presented, leading to the conclusion that the four possible classical stereoisomers of the *e,e,e* regioisomer are topologically different, and, therefore, there exist four different topological stereoisomers (*Fig. 6*). Interestingly, in the case of the *trans-3,trans-3,trans-3* tris-adduct, there are four classical stereoisomers but only two topological stereoisomers (*Fig. 7*). An example of a target molecule representing a topological *meso*-form is also presented (*Fig. 8*).

1. Introduction. – Higher covalent adducts of buckminsterfullerene (C_{60}) with interesting electrochemical [1] or chiroptical properties [2][3] are currently under intense investigation. For their synthesis, the tether-directed remote-functionalization method developed in the *Diederich* group has proved to be very powerful due to its high regio- and stereoselectivity [4]. The large variety of bis-adducts prepared by this

methodology includes enantiomerically pure *cis*-3 bis-adducts with inherently chiral functionalization pattern [2][3] and cyclophane-type fullerene crown ether [5] or porphyrin [6] conjugates, in which the second chromophore is doubly connected to the *trans*-1 positions at the two poles of the C-sphere. Fig. 1 shows the convention used to define the relative positional relationship of 6-6 bonds in multiple adducts of C₆₀ [7][8].

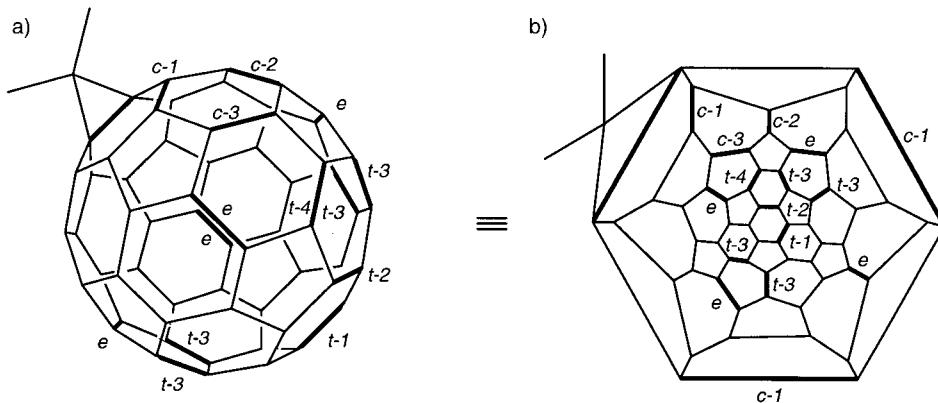
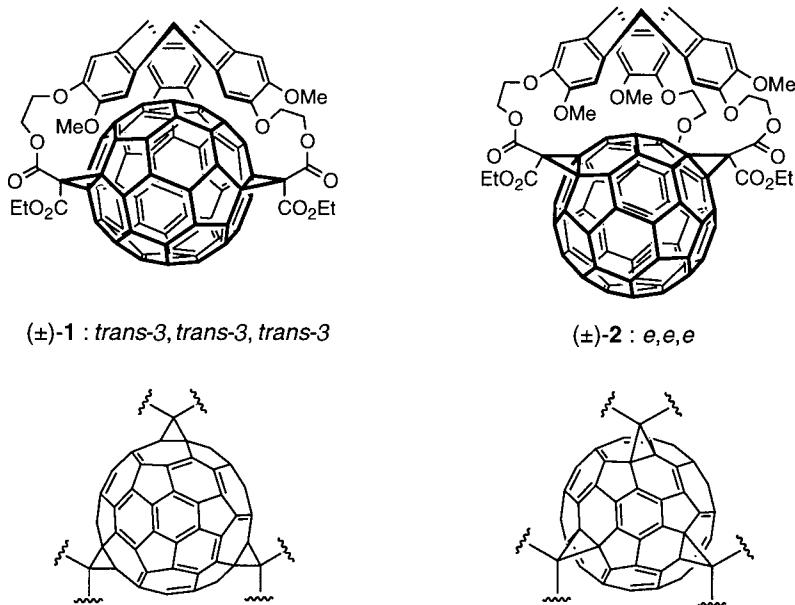


Fig. 1. Convention used to describe the positional relationship between 6-6 bonds in multiple adducts ($c = \text{cis}$, $e = \text{equatorial}$, $t = \text{trans}$) on a familiar chemical representation of C₆₀ (a) and on its planar one (b), the so-called Schlegel diagram. Shown is a monomethanofullerene derivative.

In contrast, only a few examples of tris-adducts have been described [2b][7–10]. In theory, bis-adducts of C₆₀ derived from *Bingel* cyclopropanations [11] can exist as eight different regioisomers, seven of which have been detected and isolated [7][8]. The number of possible regioisomers increases to 46 in the case of tris-adducts, in which three of the thirty 6-6 bonds (bonds between two six-membered rings) are cyclopropanated [7]. In 1994, *Hirsch et al.* reported the stepwise preparation of tris-adducts by the *Bingel* reaction and obtained the pure *trans*-3,*trans*-3,*trans*-3 and *e,e,e* regioisomers together with other isomers, after tedious separation and purification [8].

In a program aimed at expanding the scope of the tether-directed remote functionalization methodology [4], we decided to explore the preparation of tris-adducts. Here, we report the tether-directed regio- and diastereoselective synthesis of the two new C₃-symmetrical tris-adducts (\pm)-1 and (\pm)-2 with *trans*-3,*trans*-3,*trans*-3 and *e,e,e* addition patterns, respectively, in one step from C₆₀ and a tris-malonate-appended cyclotrimeratrylene (CTV) (for a preliminary communication of parts of this work, see [12]). CTV was chosen as a tether since this bowl-type molecule is well-suited in size and shape to interact favorably with C₆₀ [13][14]. The affinity between these two molecules, which is reinforced by the electron-donor character of the CTV moiety and the electron-acceptor properties of the fullerene, has been evidenced by the formation of a crystalline complex, in which C₆₀ adopts a nesting position at *van der Waals* contact distance above the concave surface of the CTV macrocycle [13a]. The electrochemical studies described here do indeed provide evidence for strong interchromophoric interactions between the CTV cap and the C-sphere in solution.



In the second part of this paper, we present a study of the chirality of CTV- C_{60} tris-adducts, such systems being not only classically but also topologically chiral. Chirality, the property of any object that is not superimposable with its mirror image, can generally be analyzed in terms of *Euclidian* geometry, on the basis of distances and angles [15][16]. The topological properties of the chemical object represent an upper level of description, leading to the notion of topological chirality. A molecule is defined to be topologically chiral if its molecular-bond graph cannot be deformed to its mirror image, even when allowing complete flexibility of the graph [17][18]. Usually, the topology of a molecule is planar. This means that the molecule can be projected onto a plane without any bond crossings. It must be clear that topological properties of molecules imply complete flexibility of their representation. At this stage, it should be noted that C_{60} itself is topologically planar, as shown by the *Schlegel* diagram in Fig. 1,*b*. On the other hand, the molecular graph of a topologically chiral molecule is necessarily non-planar. Only very few cases of such non-planar systems are known, an important family of such compounds, which consist of molecular trefoil knots, which have been prepared and resolved recently [19]. Made of a single knotted closed ring, a knot cannot be represented in a two-dimensional (2D) space without a minimum number of crossing points, three in the case of a trefoil knot. Contrary to *Euclidian* (classical) enantiomers, two topological enantiomers cannot be interconverted by a continuous deformation in a three-dimensional (3D) space without breaking a bond. According to the definition by *Frisch* and *Wasserman* [17], the left-handed trefoil knot **a** and the right-handed trefoil knot **b** are topological enantiomers and, more curiously, macrocycle **c** is their topological diastereoisomer (Fig. 2).

In contrast to the classical definition of stereoisomers, two molecules are said to be topological stereoisomers when the graph of one cannot be deformed to the graph of

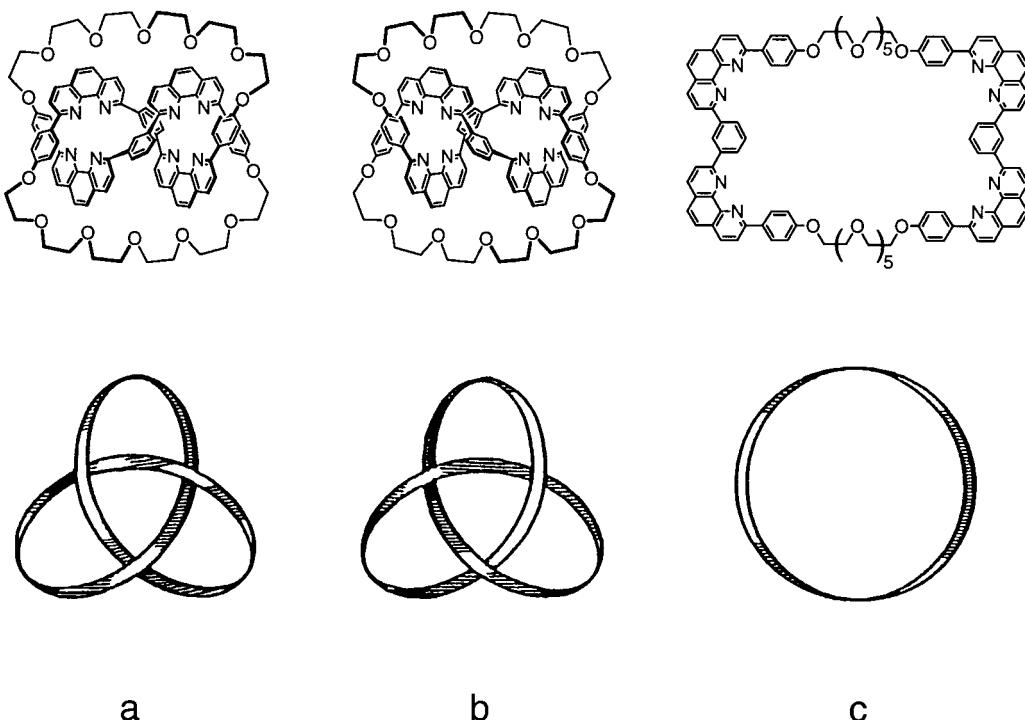
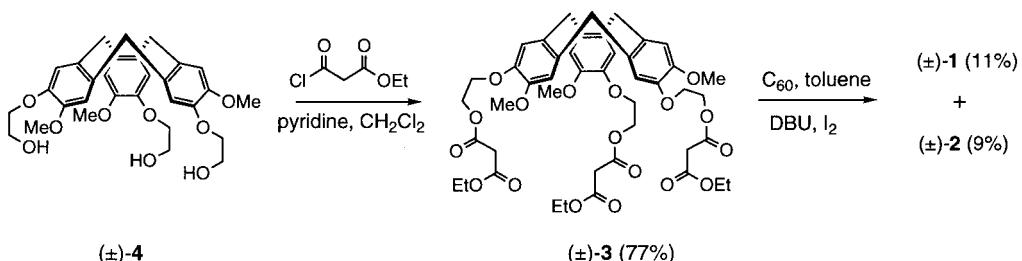


Fig. 2. Two enantiomers **a** and **b** of the trefoil knot recently resolved by Sauvage and co-workers [19] and the unknotted macrocycle **c**, which is a topological diastereoisomer of **a** and **b**

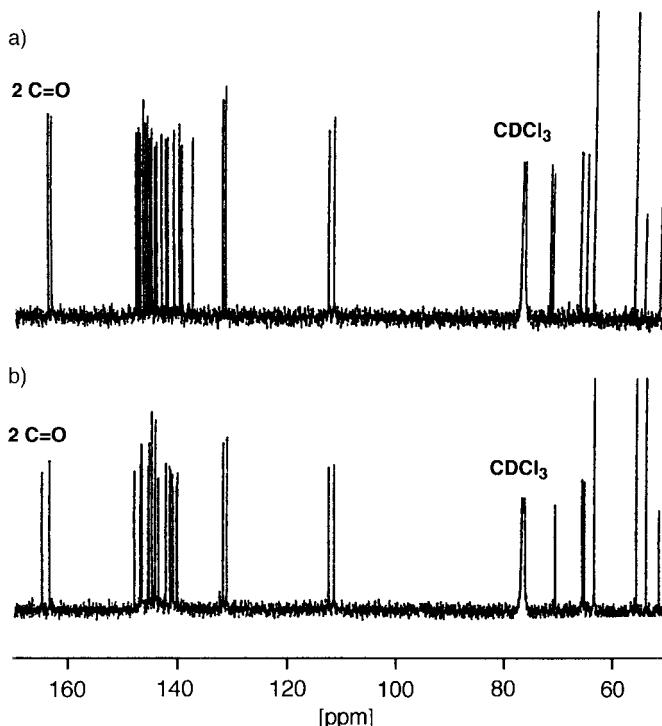
the other, even when allowing complete flexibility. In addition to proving the topological chirality of CTV-C₆₀ tris-adducts, in the second part of this paper we will analyze which of these adducts are topological stereoisomers. Also, we propose the construction of a molecule which topologically represents a *meso*-form.

2. Results and Discussion. – 2.1. *Synthesis of the Tris-adducts (\pm)-1 and (\pm)-2.* Trismalonate (\pm)-3 for the *Bingel* macrocyclization was prepared by reacting the *C*₃-symmetrical CTV derivative (\pm)-4 [20] with ethyl malonyl chloride (3.3 equiv.) at 20° in CH₂Cl₂ in the presence of pyridine (*Scheme*). After column chromatography (SiO₂; CH₂Cl₂/MeOH (0 → 1%)), (\pm)-3 was obtained in 77% yield as a colorless solid. The *Bingel* reaction of (\pm)-3 with C₆₀ was carried out in the presence of 1,8-diazabicyclo[5.4.0]undec-7-ene (DBU; 9 equiv.) and I₂ (3 equiv.). After 4 h, two products, (\pm)-1 and (\pm)-2, were formed, which were separated by column chromatography (SiO₂; CH₂Cl₂/MeOH (0 → 1%), then Al₂O₃; CH₂Cl₂) and isolated in 11 and 9% yield, respectively.

FAB Mass spectra of (\pm)-1 and (\pm)-2 displayed the molecular ions expected for the tris-adducts. The symmetry of the molecules was established by NMR spectroscopy. The ¹H-NMR spectra displayed the usual features for a *C*₃-symmetrical CTV unit, *i.e.*, two singlets for the aromatic H-atoms, one singlet for the MeO groups, and the characteristic AB quadruplets for the CH₂ bridges. This means that the adducts must

Scheme. Synthesis of the [60]Fullerene-CTV Conjugates (\pm)-1 and (\pm)-2

themselves possess a C_3 axis, which is common to the CTV and the C_{60} subunits. The ^{13}C -NMR spectra (Fig. 3), which show 20 resolved peaks for the fullerene C-atoms of (\pm)-1 and 18 for those of (\pm)-2, support this conclusion. Among all possible regioisomers, only the *trans*-3,*trans*-3,*trans*-3, and *e,e,e* tris-adducts exhibit such a symmetry (the *cis*-1,*cis*-1,*cis*-1 tris-adduct cannot form for steric reasons). On this basis, the structures of the two new tris-adducts were unambiguously established.

Fig. 3. ^{13}C -NMR Spectra (125 MHz, CDCl_3) of a) tris-adduct (\pm)-1 and b) tris-adduct (\pm)-2

Since all attempts at transesterification to give the corresponding known tris(diethyl malonate) adducts [8] failed, the structures of the two compounds were initially assigned by UV/VIS spectroscopy. Regiosomer (\pm)-1 exhibits a cherry-red color and

(\pm)-**2** an orange-red color, which are the same as those previously reported by *Hirsch et al.* [8] for the regioisomeric *trans*-3,*trans*-3,*trans*-3 and *e,e,e* tris(diethyl malonate) adducts, respectively. This difference in color is reflected in an additional absorption band at λ_{max} of 422 nm in the UV/VIS spectrum of (\pm)-**2**.

The assignment of (\pm)-**1** and (\pm)-**2** as the *trans*-3,*trans*-3,*trans*-3, and *e,e,e* isomers, respectively, was further supported by a close comparison of their NMR spectra with those of analogous untethered tris-cyclopropanated C₆₀ derivatives [8–10]. The ¹³C-NMR chemical shifts of the bridgehead sp³-C-atoms in the fullerene shell have been shown to appear at higher field in the *e,e,e* than in the *trans*-3,*trans*-3,*trans*-3 regioisomer, whereas the opposite behavior was observed for the methano-bridge C-atom. The ¹³C-NMR resonances for the cyclopropane fragments were in fact observed at 71.63, 71.11 (bridgehead), and 50.61 (bridge) ppm for (\pm)-**1** and at 70.73, 70.66 (bridgehead), and 51.07 (bridge) ppm for (\pm)-**2**. The structure assignment was further corroborated by the position of the ¹H-NMR resonance of the axial protons in the CH₂ bridges of the CTV fragment. For the tris-adduct (\pm)-**2** (4.65 ppm), this signal is nearly unaffected with respect to that observed for the free CTV (\pm)-**3** (4.74 ppm), whereas, for (\pm)-**1**, it is significantly downfield shifted to 5.33 ppm. This could indicate a much greater proximity of the CTV fragment to the fullerene core with its deshielding pentagon rings, which is expected for the *trans*-3,*trans*-3,*trans*-3 regioisomer.

It is interesting to note that the reaction proceeded with retention of symmetry, since the C₃-template yielded the two possible C₃-tris-adducts. Since a splitting and doubling of the NMR signals is observed for neither (\pm)-**1** nor for (\pm)-**2**, the triply tethered reaction is diastereoselective, and, for each of the two compounds, only one of two possible pairs of enantiomers is formed. This diastereoselectivity must still be confirmed by performing the triple *Bingel* addition with optically pure C₃-CTV **3** [21].

2.3. Electrochemical Studies. Cyclic voltammetry (CV) and *Osteryoung* square-wave voltammetry (OSWV) of (\pm)-**1** and (\pm)-**2** were carried out in CH₂Cl₂ (+0.1M Bu₄NPF₆) as described in the *Exper. Part*. Two major (quasireversible) one-electron reductions were observed for both (\pm)-**1** and (\pm)-**2** with an average potential separation of 265 mV between the two successive waves (*Fig. 4*). Also, four quasi-reversible one-electron oxidations were observed for (\pm)-**1** and two for (\pm)-**2** (*Fig. 4*). All corresponding redox potentials are reported *vs.* the ferrocene/ferricinium couple (Fc/Fc⁺) in the *Table*.

Table. Redox Potentials (*vs.* Fc/Fc⁺) for Compounds (\pm)-**1** and (\pm)-**2** Obtained by CV and OSWV

	E _{red} ¹	E _{red} ²	E _{ox} ¹	E _{ox} ²	E _{ox} ³	E _{ox} ⁴
(\pm)- 1	–1.37	–1.63	0.81	0.99	1.23	1.41
(\pm)- 2	–1.40	–1.67	0.79	0.98	n.o. ^{a)}	n.o. ^{a)}

^{a)} Not observed.

Scanning to more negative potentials showed the appearance of two additional very small reduction waves at –1.86 and –2.09 V for (\pm)-**1** and at –1.87 and –2.07 for (\pm)-**2**. These third and fourth reductions, which exhibit a much smaller current than the first and second, may correspond to the reduction of products that are formed as a consequence of the initial reduction of (\pm)-**1** and (\pm)-**2**, since we observed that their

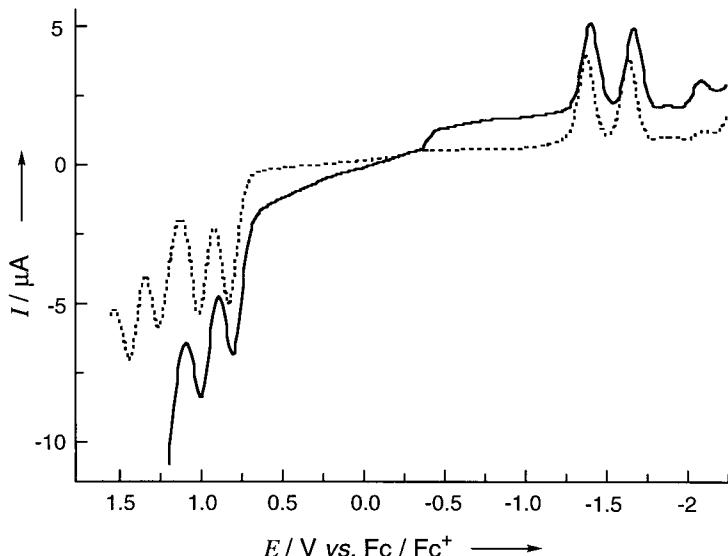


Fig. 4. OSWV of (\pm) -**1** (dotted line) and (\pm) -**2** (solid line) in CH_2Cl_2 . Step = 4 mV; Amplitude = 25 mV; Frequency = 15 Hz.

intensity varies as a function (CV) scan rate. This indicates the presence of an ECE (electrochemical electron transfer/chemical reaction/electrochemical electron transfer) mechanism, a possibility in view of similar behavior reported previously for bis-malonate adducts of C_{60} [22]. More interesting, however, is the observation that the first and second reduction potentials are by exactly 100 mV more negative than those of their corresponding tris[bis(ethoxycarbonyl)methano][60]fullerene analogs with the respective *trans-3,trans-3,trans-3* and *e,e,e* addition patterns [23]. In both (\pm) -**1** and (\pm) -**2**, the donor-acceptor interaction between the CTV and the fullerene chromophores apparently strongly influence the electrochemical behavior. Another interpretation of the 100-mV shifts of the first fullerene-centered reduction potentials is based on environmental changes created by the CTV cap. In the two conjugates, the convex fullerene surface, characterized by a large positive molecular electrostatic potential, is surrounded by the complementary concave aromatic surfaces of the CTV cap. Such concave surfaces are characterized by a particularly large negative molecular electrostatic potential [24] that could render the fullerene-centered first reduction step more difficult. Both the CTV-conjugate (\pm) -**1** and the corresponding *trans-3,trans-3,trans-3* tris(diethyl malonate) are by 30 mV easier to reduce than conjugate (\pm) -**2** and the corresponding *e,e,e* tris(diethyl malonate), respectively. This potential difference must result from the different electronic configuration created by the two addition patterns. The fact that the CTV cap affects the reduction potential in the same way in both conjugates suggests that the average interchromophoric distance is similar in both compounds. The different interchromophoric orientation in the two conjugates, which is evidenced by the differential $^1\text{H-NMR}$ shifts of the axial protons in the CTV CH_2 bridges (see above), apparently does not affect the redox properties.

2.4. Chirality and Topological Chirality of the CTV Tris-adducts. The chirality of (\pm)-**1** and (\pm)-**2** is generated by both the chirality of the CTV cap and the chiral addition pattern. Classically, two stereogenic elements yield a maximum of four stereoisomers. They are represented in Fig. 6 for the *e,e,e* regioisomer and in Fig. 7 for the *trans-3,trans-3,trans-3* and regioisomer (see below). Topologically, the analysis is not straightforward, and the evidence for the topological chirality of a molecule and the number of stereoisomers require a complete mathematical demonstration.

In the case of molecules, the property ‘topology’ may have two different meanings [18]: the *intrinsic* topology of a molecule is simply its atom connectivity. The *extrinsic* topology of a molecule appears when the molecule in consideration is embedded in a three-dimensional space.

When the molecule is said to be non-planar, this means that it is not possible to find a projection which presents no crossings between bonds. This can be achieved intrinsically or extrinsically. Intrinsically non-planar molecules have connectivity patterns, also called molecular graphs, which can be basically reduced to either two graphs containing a single crossing: these patterns are known as the *Kuratowski* graphs K_5 and $K_{3,3}$ (Fig. 5). In the case of K_5 , five points are connected to each other; in the case of $K_{3,3}$, two sets of three points each are interconnected. Examples of molecules with such graphs are the centrally annelated polyquinane derivative with a K_5 connectivity [25] and the triple-decker naphthalenophane, which gives a $K_{3,3}$ graph [26] (Fig. 5). Extrinsically topologically non-planar molecules do not owe their non-planarity to their molecular graph, they contain, for example, the knotted structures shown in Fig. 2.

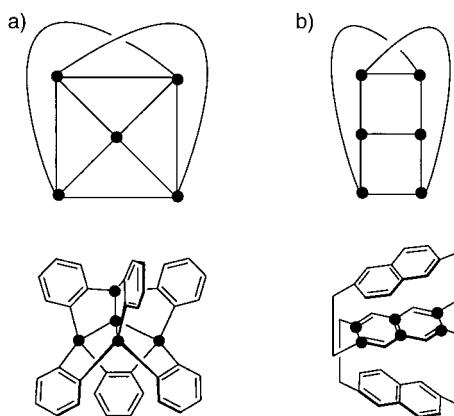


Fig. 5. The Kuratowski graphs K_5 (a) and $K_{3,3}$ (b) (top) and examples of molecules with such graphs (bottom)

A graph in 3D space is said to be *topologically chiral*, if it cannot be deformed to its mirror image, even if it is completely flexible. A graph G is said to be *intrinsically chiral*, if every embedding of the graph in 3D space is topologically chiral. Any molecular graph that is intrinsically chiral is necessarily topologically chiral. To show that the molecular graphs of the CTV tris-adducts of C_{60} with *trans-3,trans-3,trans-3* and with *e,e,e* addition patterns are topologically chiral, we shall prove that they are intrinsically chiral. To do this, we will use the result that any non-planar graph that has no order-two

automorphism must be intrinsically chiral [27]. We observe that the graphs of both $(\pm)\textbf{1}$ and $(\pm)\textbf{2}$ are non-planar, since they each contain the bipartite graph $K_{3,3}$ as a subgraph. An *automorphism* of a graph is a permutation of the vertices, which takes adjacent vertices to adjacent vertices. Any symmetry of a graph in space induces an automorphism on the vertices of the graph; however, not all automorphisms of a graph necessarily come from symmetries of the graph in space. An automorphism is said to be of *order n* if performing it n times returns every vertex to its original position, yet performing it fewer than n times does not. Any automorphism of one of these tris-adduct graphs must take the C_{60} subunit to itself and the CTV subunit to itself. The CTV subunit has no automorphism of order two, so if there is an order-two automorphism of one of the adducts, then it must fix every vertex of the CTV subunit.

For the tris-adduct with e,e,e addition pattern, there is a unique circuit of 15 edges in the C_{60} subunit that contains the six vertices at which the CTV subunit is attached to the C-sphere. Any automorphism that fixes these six vertices must fix every vertex of this circuit. As there are fewer of the C_{60} vertices inside this circuit than outside of it, any automorphism that fixes every vertex of this circuit must fix every vertex of the tris-adduct, and hence have order one. Thus the tris-adduct with e,e,e pattern cannot have an automorphism of order two, and, hence, is intrinsically chiral. For the tris-adduct with *trans-3,trans-3,trans-3* addition pattern, the six vertices where the CTV subunit is attached lie along a unique equatorial circuit of 18 edges. Any automorphism that fixes these six vertices must fix every vertex of this circuit. However, each vertex along this circuit has precisely one incident edge in the C_{60} that is not on the circuit. Thus, any automorphism that fixes every vertex of this circuit must also fix each of these incident edges. This implies that any such automorphism must fix every vertex of the tris-adduct, and hence have order one. Therefore, the tris-adduct with *trans-3,trans-3,trans-3* pattern cannot have an automorphism of order two, and hence is intrinsically chiral. It follows that both tris-adducts must be topologically chiral.

2.4.1. Number of Topological Stereoisomers for the e,e,e Tris-adduct. We will denote the first pair of enantiomers of the tris-adduct with the e,e,e addition pattern by \mathbf{G}_1 and \mathbf{G}_2 (Fig. 6), and the second pair of enantiomers by \mathbf{G}_3 and \mathbf{G}_4 . Since \mathbf{G}_1 is topologically chiral, we know that \mathbf{G}_1 cannot be deformed to \mathbf{G}_2 . We shall prove that \mathbf{G}_1 cannot be deformed to either \mathbf{G}_3 or \mathbf{G}_4 . We define a homeomorphism of 3D space as a continuous function of 3D space that has a continuous inverse. If \mathbf{G}_1 could be deformed to \mathbf{G}_3 , then the deformation gives us a homeomorphism of 3D space that takes \mathbf{G}_1 to \mathbf{G}_3 . If \mathbf{G}_1 could be deformed to \mathbf{G}_4 , then, by composing this deformation with a reflection of 3D space, we also obtain a homeomorphism of 3D space that takes \mathbf{G}_1 to \mathbf{G}_3 . We will show that there can be no homeomorphism of 3D space that takes \mathbf{G}_1 to \mathbf{G}_3 , thus showing that \mathbf{G}_1 cannot be deformed to either \mathbf{G}_3 or \mathbf{G}_4 .

Suppose that there were a homeomorphism h , of 3D space that takes \mathbf{G}_1 to \mathbf{G}_3 . Then, h takes the C_{60} of \mathbf{G}_1 to the C_{60} of \mathbf{G}_3 , and the CTV subunit of \mathbf{G}_1 to the CTV subunit of \mathbf{G}_3 . Let T_1 denote the unique circuit of 21 edges going around the outside of the CTV subunit of \mathbf{G}_1 , and let T_3 denote the comparable circuit on \mathbf{G}_3 . We draw an arrow on one of the edges of T_1 that goes from where an O-atom (from the linker to the fullerene) is attached to where the adjacent MeO group is attached, and we draw a similar arrow on T_3 . These arrows give orientations to the circuits T_1 and T_3 . Hence, looking down on \mathbf{G}_1 from above its CTV subunit, we see that T_1 is oriented in the

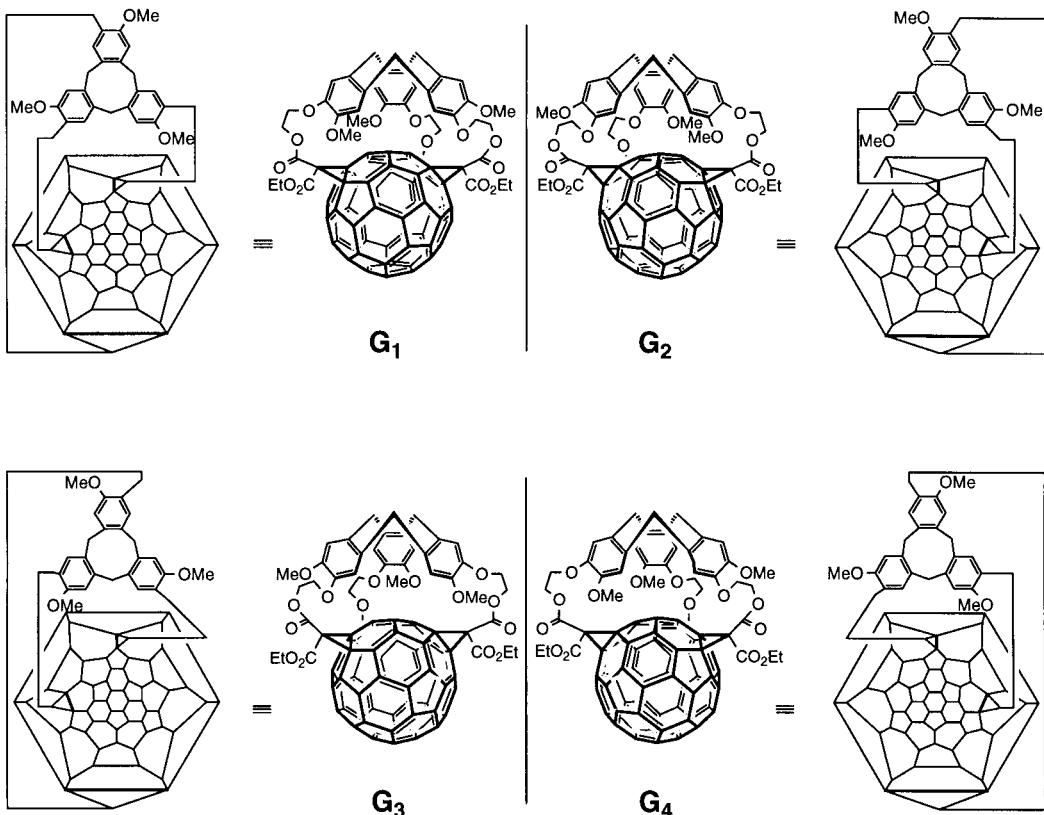


Fig. 6. The four classical stereoisomers of the e,e,e-CTV- C_{60} tris-adduct and their planar representations. **G₁**, **G₂**, **G₃**, and **G₄** are four different topological stereoisomers. The vertical line represents the virtual mirror between each pair of enantiomers.

counterclockwise direction; and looking down on **G₃** from above its CTV subunit, we see that T_3 is oriented in the clockwise direction. Since h must take each O-atom to an O-atom and each MeO group to a MeO group, h must take the oriented T_1 to the oriented T_3 .

Let C_1 denote the unique circuit of 15 edges in the C_{60} of **G₁** that contains the six vertices at which the CTV subunit is attached, and let C_3 denote the comparable circuit in **G₃**. Then, h takes C_1 to C_3 . Let L_1 denote the structure that we obtain by taking T_1 together with C_1 , as well as the three linkages between the CTV subunit and the C_{60} , and let L_3 denote the comparable structure in **G₃**. Then, L_1 and L_2 each have the form of a closed circular three-rung ladder, and the arrows on T_1 and T_3 induce parallel arrows on C_1 and C_3 . Now, h takes L_1 to L_2 , and it follows that h takes the oriented C_1 to the oriented C_3 . Observe that C_1 and C_3 represent the same circuit on C_{60} ; however, C_1 is oriented counterclockwise, and C_3 is oriented clockwise. Thus, h takes the C_{60} of **G₁** to the C_{60} of **G₃**, taking this particular circuit to itself reversing its orientation. Furthermore, h must take pairs of vertices where the CTV subunit is attached to similar pairs of vertices. However, since h reverses the orientation of this circuit, this

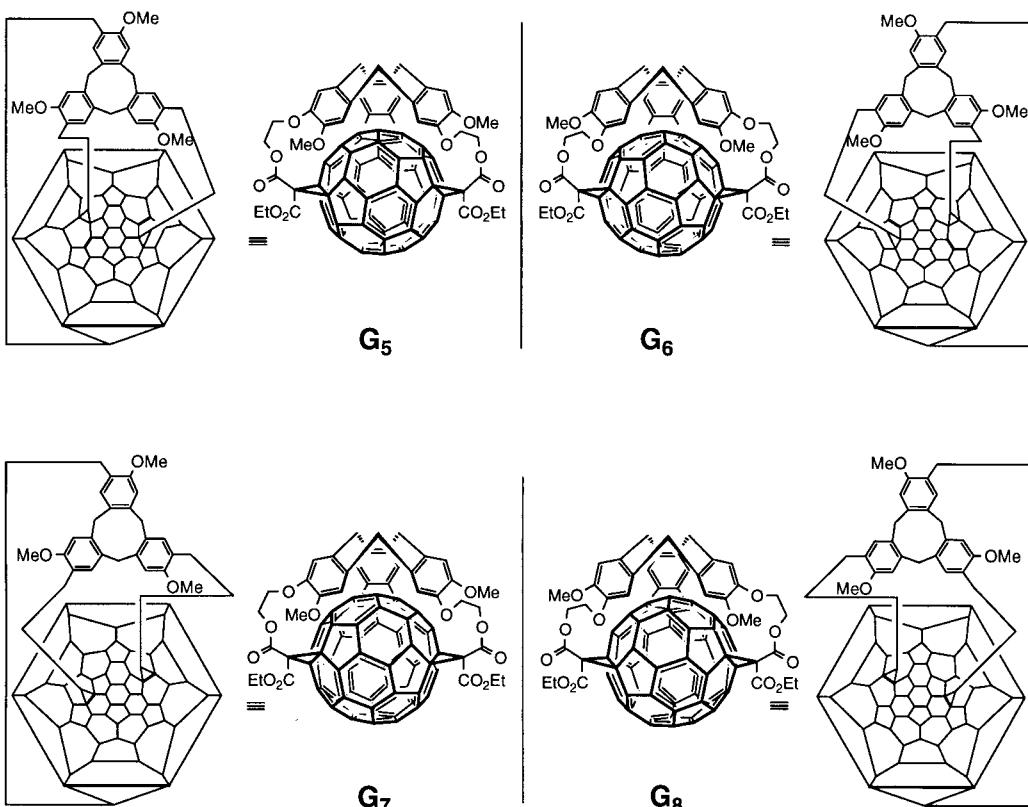


Fig. 7. The four classical stereoisomers of the trans-3,trans-3,trans-3-CTV- C_{60} tris-adduct and their planar representations. Topologically, \mathbf{G}_5 is equivalent (can be deformed without breaking any bond) to \mathbf{G}_8 , and \mathbf{G}_6 is equivalent to \mathbf{G}_7 . It seems that four classical stereoisomers are reduced to only two different topological stereoisomers. The vertical line represents the virtual mirror between each pair of enantiomers.

implies that h takes an edge shared by two hexagons to an edge shared by a hexagon and a pentagon. As this is impossible, no such homeomorphism h could exist. It follows that \mathbf{G}_1 cannot be deformed to either \mathbf{G}_3 or \mathbf{G}_4 . Therefore, in the case of the e,e,e tris-adduct enantiomers, it is not possible to deform one pair of enantiomers to the other, even if we were to make the graphs completely flexible. Hence, the four classical stereoisomers of the e,e,e tris-adduct are all topological stereoisomers.

2.4.2. Number of Topological Stereoisomers for the trans-3,trans-3,trans-3 Tris-adduct. In the case of the *trans*-3,trans-3,trans-3 regioisomer, it can be shown that the enantiomer \mathbf{G}_5 can be deformed to diastereoisomer \mathbf{G}_8 , if we allow complete flexibility of the graph (Fig. 7). To deform \mathbf{G}_5 into \mathbf{G}_8 , we have to stretch the nine-membered ring in the CTV subunit of \mathbf{G}_5 so that it becomes so large that the C_{60} can pass through the center of the ring. Then, push the C_{60} up through the center of this ring so that the C_{60} is now on the top and the CTV subunit is on the bottom, and we obtain \mathbf{G}_8 .

An analogous deformation exists between the diastereoisomers \mathbf{G}_6 and \mathbf{G}_7 . Of course, these deformations cannot occur on a chemical level, but they exist topo-

logically. Hence, there are four classical stereoisomers but only two topological stereoisomers.

2.4.3. An Example of a Topological meso-Form. For symmetry reasons, there can be fewer stereoisomers than expected for a certain number of stereogenic elements. The most classical example is the presence of an internal mirror plane that gives rise to a *meso*-form. Here, $(\pm)\text{-1}$ and $(\pm)\text{-2}$ have two stereogenic elements (the CTV fragment and the addition pattern on the fullerene), which yield four classical stereoisomers, but, topologically, $(\pm)\text{-1}$ has not four but two stereoisomers. This arises, like for classical *meso*-forms, from the higher symmetry of $(\pm)\text{-1}$, compared to $(\pm)\text{-2}$. From the point of view of the C-atoms of the C_{60} fragment, $(\pm)\text{-1}$ is cut in two equal parts by the position of the addition patterns, whereas in $(\pm)\text{-2}$ the two parts are different. Therefore, when we stretch the nine-membered ring in the CTV subunit to pass the fullerene fragment through the center of the ring, the product of the deformation is topologically identical, this is not the case for $(\pm)\text{-2}$. However, $(\pm)\text{-1}$ is not a *meso*-form at the topological level, since $(\pm)\text{-1}$ is topologically chiral. It must be noted here that a *meso*-form is necessarily achiral, so a topological *meso*-form must be topologically achiral. With this aim in view, we could imagine a molecule directly derived from $(\pm)\text{-1}$, which would be a true topological *meso*-form. This molecule (*Fig. 8*) is made from $(\pm)\text{-1}$ with a second CTV fragment of the same chirality, capping the opposite pole of the C-sphere.

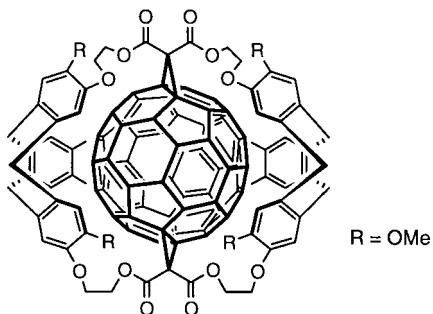


Fig. 8. An example of a hypothetical molecule in a topological meso-form. The addition pattern on the fullerene is *trans*-3,*trans*-3,*trans*-3.

3. Conclusion. – The tether-directed triple *Bingel* addition of $(\pm)\text{-3}$ to C_{60} provided the *trans*-3,*trans*-3,*trans*-3 tris-adduct $(\pm)\text{-1}$ (11%) and the *e,e,e* regioisomer $(\pm)\text{-2}$ (9%) in a total yield of 20%. Given the expected low statistical yields (0.5% for *trans*-3,*trans*-3,*trans*-3 and 1% for *e,e,e*), one can assume that the CTV template is largely responsible for this high degree of regioselectivity. Both compounds possess two stereogenic elements that come from the CTV cap and the chiral addition pattern on the fullerene, and, therefore, each can be formed, in principle, as a mixture of two diastereomeric pairs of enantiomers. However, the NMR data provide very good evidence that each regioisomer is obtained as only one pair of enantiomers, suggesting that the triply tethered addition is highly diastereoselective. This will be further confirmed in future work by performing the addition with optically active CTV-precursor **3**. Electrochemical investigations show a strong interchromophoric interaction between the electron-rich CTV cap and the electron-deficient fullerene moiety in both tris-adducts:

the potential for the first fullerene-centered reduction in these compounds is by 100 mV more negative than in the corresponding tris(diethyl malonate) adducts, which lack the CTV cap. Additional interest arises from the fact that both (\pm) -**1** and (\pm) -**2** are topologically chiral. A complete topology study leads to the conclusion that the four classical stereoisomers of the *e,e,e* regioisomer are four different topological stereoisomer, whereas, in the case of the *trans-3,trans-3,trans-3* tris-adduct, there are four classical stereoisomers but only two topological stereoisomers. A *trans-3,trans-3,trans-3* [60]fullerene tris-adduct with two CTV caps of identical chirality is presented as a target molecule representing a topological *meso*-form, and this fascinating compound is currently under preparation. Finally, the introduction of topological isomerism adds another milestone to the ongoing exploration of the chirality of fullerenes and their covalent and supramolecular derivatives, an exciting field of contemporary stereochemistry [28].

Experimental Part

General. Reagents and solvents were purchased reagent grade and used without further purification. CH_2Cl_2 was dried over CaH_2 , pyridine over KOH. CTV (\pm)-**4** was prepared according to the literature [20]. C_{60} (99.5%) was purchased from *Southern Chemical Group*. All reactions were carried out in standard glassware under Ar. Evaporation and concentration were performed at water-aspirator pressure, and compounds were dried at 10^{-2} Torr. Column chromatography (CC): Al_2O_3 (basic), activity I from *Woelm Pharma*: SiO_2 60 (230–400 mesh, 0.040–0.063 mm) from *E. Merck*. UV/VIS Spectra (λ_{max} in nm (ϵ [$1 \text{ mol}^{-1} \text{ cm}^{-1}$]): *Varian Cary 5* spectrophotometer. IR Spectra [cm^{-1}]: *Perkin-Elmer 1600-FTIR*. NMR Spectra: *Bruker AMX 500* and *Varian Gemini 200* at 300 K with solvent peak as reference. FAB-MS: *VG ZAB2-SEQ* instrument: 3-nitrobenzyl alcohol as matrix; positive-ion mode. Elemental analyses were performed by the Mikrolabor at the Laboratorium für Organische Chemie, ETH Zürich.

(\pm) -*I,I,I'-Triethyl 3,3',3'-(3,8,13-Trimethoxy-10,15-dihydro-5H-tribenzo[a,d,g]cyclononene-2,7,12-triyltris/oxy(ethan-1,2-diyl)) Tris(propanedioate) ((\pm)-**3**). Ethyl 3-chloro-3-oxopropanoate (84 mg, 71 μl , 550 μmol) was added under Ar to a stirred soln. of (\pm)-**4** (50 mg, 92.5 μmol) and pyridine (44 mg, 45 μl , 550 μmol) in freshly distilled CH_2Cl_2 (150 ml). After 15 min, the temp. was raised to 20°, and the mixture was stirred overnight. The mixture was washed with sat. aq. NH_4Cl soln. (3 \times 100 ml) and sat. aq. Na_2CO_3 soln. (3 \times 100 ml) and dried (MgSO_4). Evaporation and CC (SiO_2 ; $\text{CH}_2\text{Cl}_2/\text{MeOH}$ (0–2%)) provided (\pm)-**3** (63 mg, 77%). Colorless amorphous solid. IR (KBr): 1749 (C=O). $^1\text{H-NMR}$ (CDCl_3 , 200 MHz): 6.93 (s, 3 H); 6.87 (s, 3 H); 4.74 (d, $J = 13.9, 3$ H); 4.45 (q, $J = 7.0, 6$ H); 4.20 (m, 12 H); 3.83 (s, 9 H); 3.55 (d, $J = 13.9, 3$ H); 3.39 (s, 6 H); 1.25 (t, $J = 7.0, 9$ H). $^{13}\text{C-NMR}$ (CDCl_3 , 125 MHz): 166.62; 166.31; 148.88; 146.51; 133.46; 131.84; 117.17; 114.05; 67.50; 63.61; 61.54; 56.22; 41.35; 36.35; 13.90. FAB-MS: 905.2 (91, $[M + \text{Na}]^+$), 882.2 (100, M^+).*

*Reaction of (\pm)-**3** with C_{60} .* DBU (69 μl , 450 μmol) was added under Ar at 20° to a well-degassed soln. of C_{60} (37 mg, 51 μmol), I_2 (41 mg, 162 μmol), and (\pm)-**3** (45 mg, 51 μmol) in toluene (150 ml). The mixture was stirred for 4 h and filtered through a short plug (SiO_2), first eluting with toluene to remove unreacted C_{60} and then with $\text{CH}_2\text{Cl}_2/\text{MeOH}$ 98:2. CC (SiO_2 ; $\text{CH}_2\text{Cl}_2/\text{MeOH}$ (0–1%)) separated traces of other brown-colored tris-adducts from the red mixture of (\pm)-**1** and (\pm)-**2**. CC (Al_2O_3 ; CH_2Cl_2) afforded (\pm)-**1** (9.0 mg, 11%) and (\pm)-**2** (7.7 mg, 9%).

(\pm) -out,out,out-*61,62,63-Triethyl 61,62,63-[3,8,13-Trimethoxy-10,15-dihydro-5H-tribenzo[a,d,g]cyclonene-2,7,12-triyltris/oxy(ethan-1,2-diyl)]-1,2:33,50:41,42-Tris(methano)[60]fullerene-61,61,62,62,63,63-hexacarboxylate (\pm)-**1**: Cherry-red solid. M.p. >250°. UV/VIS (CH_2Cl_2): 297 (33100), 316 (sh, 25500); 488 (2810); 570 (sh, 1250). $^1\text{H-NMR}$ (CDCl_3 , 500 MHz): 6.61 (s, 3 H); 6.55 (s, 3 H); 5.33 (d, $J = 12.5, 3$ H); 4.63 (m, 6 H); 4.45 (q, $J = 7.1, 6$ H); 4.13 (m, 3 H); 4.02 (m, 3 H); 3.63 (s, 9 H); 3.37 (d, $J = 12.5, 3$ H); 1.42 (t, $J = 7.1, 9$ H). $^{13}\text{C-NMR}$ (CDCl_3 , 125 MHz): 164.13; 163.55; 148.36; 147.89; 147.59; 147.06; 146.69; 146.31; 145.97; 145.73; 145.68; 145.53; 144.97; 144.67; 143.74; 143.00; 142.66; 141.64; 141.49; 140.60; 140.14; 138.16; 132.67; 132.11; 113.17; 112.15; 71.63; 71.11; 65.80; 64.65; 63.32; 55.42; 53.41; 50.61; 14.10. HR-FAB-MS: 1596.2839 (M^+ , $\text{C}_{105}\text{H}_{48}\text{O}_{18}^+$; calc. 1596.2841).*

(\pm) -out,out,out-*61,62,63-Triethyl 61,62,63-[3,8,13-Trimethoxy-10,15-dihydro-5H-tribenzo[a,d,g]cyclonene-2,7,12-triyltris/oxy(ethan-1,2-diyl)]-1,2:18,36:22,23-Tris(methano)[60]fullerene-61,61,62,62,63,63-hexa-*

carboxylate (±)-2: Orange-red solid. M.p. >250°. UV/VIS (CH₂Cl₂): 296 (43600); 319 (sh, 30000); 422 (2450); 486 (3270); 568 (sh, 1550). ¹H-NMR (CDCl₃, 500 MHz): 6.56 (s, 3 H); 6.53 (s, 3 H); 4.93 (m, 3 H); 4.82 (m, 3 H); 4.65 (d, J=14.5, 3 H); 4.47 (q, J=7.1, 6 H); 4.15 (m, 6 H); 3.58 (s, 9 H); 3.38 (d, J=14.5, 3 H); 1.40 (t, J=7.1, 9 H). ¹³C-NMR (CDCl₃, 125 MHz): 164.96; 163.57; 148.32; 147.44; 147.34; 147.14; 146.95; 146.02; 145.73; 145.22; 144.78; 144.58; 144.10; 142.69; 142.06; 141.89; 141.55; 141.40; 140.87; 140.62; 132.32; 131.65; 112.93; 111.95; 70.73; 70.66; 65.53; 65.10; 63.30; 55.24; 53.40; 51.07; 14.10. HR-FAB-MS: 1596.2835 (M^+ , C₁₀₅H₄₈O₁₈; calc. 1596.2841).

Electrochemical Experiments. CV and OSWV were performed on a Windows-driven *BAS 100W* electrochemical analyzer (*Bioanalytical Systems*, West Lafayette, IN) at 20° in CH₂Cl₂ containing the substrate (0.1–0.5 mmol dm⁻³) and Bu₄NPF₆ (0.1 mol dm⁻³) as supporting electrolyte. A three-electrode configuration, consisting of a glassy C disc (GC, 3 mm) as working, a Pt wire (1 mm) as counter, and an Ag wire (1 mm) as pseudo-reference electrodes, was used. The surface of the working electrode was polished prior to each measurement with commercial *Alpha Micropolish Alumina* (*Aldrich*) with a particle size of 0.05 μ. Bu₄NPF₆ (98%) was purchased from *Fluka*, recrystallized twice from EtOH, and dried in high vacuum (10⁻⁶ Torr). CH₂Cl₂ (HPLC grade) was purchased from *Aldrich*, further purified by drying with P₂O₅ and vapor-transferred under vacuum (10⁻⁶ Torr). Solns. were stirred and degassed with Ar prior to each voltammetric measurement. For CV, scan rates were 100 to 800 mV s⁻¹. OSWV was performed with an amplitude of 25 mV, a frequency of 15 Hz, and a step potential of 4 mV.

This work was supported by the *Swiss National Science Foundation*, the *CNRS*, and the *US National Science Foundation* (CHE-9816503). G. R. is grateful for a *Lavoisier* postdoctoral fellowship of the *French Ministry of Foreign Affairs*.

REFERENCES

- [1] L. Echegoyen, L. E. Echegoyen, *Acc. Chem. Res.* **1998**, *31*, 593.
- [2] a) J.-F. Nierengarten, V. Gramlich, F. Cardullo, F. Diederich, *Angew. Chem.* **1996**, *108*, 2242; *Angew. Chem., Int. Ed.* **1998**, *35*, 2101; b) J.-F. Nierengarten, T. Habicher, R. Kessinger, F. Cardullo, F. Diederich, V. Gramlich, J.-P. Gisselbrecht, C. Boudon, M. Gross, *Helv. Chim. Acta* **1997**, *80*, 2238.
- [3] H. Isobe, H. Tokuyama, M. Sawamura, E. Nakamura, *J. Org. Chem.* **1997**, *62*, 5034; M. Taki, Y. Nakamura, H. Uehara, M. Sato, J. Nishimura, *Enantiomer* **1998**, *3*, 231.
- [4] F. Diederich, R. Kessinger, *Acc. Chem. Res.* **1999**, *32*, 537; F. Diederich, R. Kessinger in ‘Templated Organic Synthesis’, Eds. F. Diederich, P. J. Stang, Wiley-VCH, Weinheim, 2000, pp. 189–218.
- [5] J.-P. Bourgeois, L. Echegoyen, M. Fibbioli, E. Pretsch, F. Diederich, *Angew. Chem.* **1998**, *110*, 2203; *Angew. Chem., Int. Ed.* **1998**, *37*, 2118; J.-P. Bourgeois, P. Seiler, M. Fibbioli, E. Pretsch, F. Diederich, L. Echegoyen, *Helv. Chim. Acta* **1999**, *81*, 1572.
- [6] J.-P. Bourgeois, F. Diederich, L. Echegoyen, J.-F. Nierengarten, *Helv. Chim. Acta* **1998**, *81*, 1835; see also: E. Dietel, A. Hirsch, E. Eichhorn, A. Rieker, S. Hackbarth, B. Röder, *Chem. Commun.* **1998**, 1981.
- [7] A. Hirsch, *Top. Curr. Chem.* **1999**, *199*, 1.
- [8] A. Hirsch, I. Lamparth, H. R. Karfunkel, *Angew. Chem.* **1994**, *116*, 453; *Angew. Chem., Int. Ed.* **1994**, *33*, 437.
- [9] A. Hirsch, I. Lamparth, T. Grösser, H. R. Karfunkel, *J. Am. Chem. Soc.* **1994**, *116*, 9385; T. Hamano, K. Okuda, T. Mashino, M. Hirobe, K. Arakane, A. Ryu, S. Mashiko, T. Nagano, *Chem. Commun.* **1997**, *21*; F. Djojo, A. Hirsch, *Chem. Eur. J.* **1998**, *4*, 344; F. Djojo, A. Hirsch, S. Grimme, *Eur. J. Org. Chem.* **1999**, 3027.
- [10] L. Isaacs, F. Diederich, R. F. Haldimann, *Helv. Chim. Acta* **1997**, *80*, 317; F. Cardullo, P. Seiler, L. Isaacs, J.-F. Nierengarten, R. F. Haldimann, F. Diederich, T. Mordasini-Denti, W. Thiel, C. Boudon, J.-P. Gisselbrecht, M. Gross, *Helv. Chim. Acta* **1997**, *80*, 343.
- [11] C. Bingel, *Chem. Ber.* **1993**, *126*, 1957.
- [12] G. Rapenne, J. Crassous, A. Collet, L. Echegoyen, F. Diederich, *Chem. Commun.* **1999**, 1121.
- [13] a) J. W. Steed, P. C. Junk, J. L. Atwood, M. J. Barnes, C. L. Raston, R. S. Burkhalter, *J. Am. Chem. Soc.* **1994**, *116*, 10346; b) J. L. Atwood, M. J. Barnes, M. G. Gardiner, C. L. Raston, *Chem. Commun.* **1996**, 1449.
- [14] H. Matsubara, A. Hasegawa, K. Shiwaku, K. Asano, M. Uno, S. Takahashi, K. Yamamoto, *Chem. Lett.* **1998**, 923; H. Matsubara, S. Y. Oguri, K. Asano, K. Yamamoto, *Chem. Lett.* **1999**, 431.
- [15] R. S. Cahn, C. Ingold, V. Prelog, *Angew. Chem.* **1966**, *78*, 413; *Angew. Chem., Int. Ed.* **1966**, *5*, 385; E. L. Eliel, S. H. Wilen, ‘Stereochimistry of Organic Compounds’, 2nd edn., Wiley, New York, 1994.
- [16] K. Mislow, *Bull. Soc. Chim. Belg.* **1977**, *86*, 595; K. Mislow, J. Siegel, *J. Am. Chem. Soc.* **1984**, *106*, 3319.

- [17] H. L. Frisch, E. Wasserman, *J. Am. Chem. Soc.* **1961**, *83*, 3789.
- [18] D. M. Walba, *Tetrahedron* **1985**, *41*, 3161; J.-C. Chambron, C. O. Dietrich-Buchecker, J.-P. Sauvage, *Top. Curr. Chem.* **1993**, *165*, 131; C. Liang, K. Mislow, *J. Math. Chem.* **1994**, *15*, 245; G. A. Breault, C. A. Hunter, P. C. Mayers, *Tetrahedron* **1999**, *55*, 5265.
- [19] G. Rapenne, C. O. Dietrich-Buchecker, J.-P. Sauvage, *J. Am. Chem. Soc.* **1996**, *118*, 10932; J.-C. Chambron, C. O. Dietrich-Buchecker, G. Rapenne, J.-P. Sauvage, *Chirality* **1998**, *10*, 125; C. Dietrich-Buchecker, G. Rapenne, J.-P. Sauvage, ‘Molecular Catenanes, Rotaxanes and Knots’, Wiley-VCH, Weinheim, 1999, 107; C. Dietrich-Buchecker, G. Rapenne, J.-P. Sauvage, A. De Cian, J. Fischer, *Chem. Eur. J.* **1999**, *5*, 1432.
- [20] J. Canceill, J. Gabard, A. Collet, *J. Chem. Soc., Chem. Commun.* **1983**, 122; J. Canceill, J. Gabard, A. Collet, *J. Am. Chem. Soc.* **1984**, *106*, 5997; G. Vériot, J.-P. Dutasta, G. Matouzenko, A. Collet, *Tetrahedron* **1995**, *51*, 389.
- [21] A. Collet, in ‘Comprehensive Supramolecular Chemistry’, Vol. 6, Ed. F. Toda, Pergamon, 1996, Chapt. 9, pp. 281–303.
- [22] R. Kessinger, M. Gómez-López, C. Boudon, J.-P. Gisselbrecht, M. Gross, L. Echegoyen, F. Diederich, *J. Am. Chem. Soc.* **1998**, *120*, 8545.
- [23] L. E. Echegoyen, F. Djojo, A. Hirsch, L. Echegoyen, unpublished results.
- [24] M. Kamieth, F.-G. Klärner, F. Diederich, *Angew. Chem.* **1998**, *110*, 3497; *Angew. Chem. Int. Ed.* **1998**, *37*, 3303; F. Diederich, M. Goméz-Lopez, *Chem. Soc. Rev.* **1999**, *28*, 263.
- [25] D. Kuck, A. Schuster, *Angew. Chem.* **1988**, *100*, 1222; *Angew. Chem., Int. Ed.* **1988**, *27*, 1192.
- [26] T. Otsubo, F. Ogura, S. Misumi, *Tetrahedron Lett.* **1983**, *24*, 4851; T. Otsubo, Y. Aso, F. Ogura, S. Misumi, A. Kawamoto, J. Tanaka, *Bull. Chem. Soc. Jpn.* **1989**, *62*, 164.
- [27] E. Flapan, *J. of Knot Theory and its Ramifications* **1995**, *4*, 373.
- [28] C. Thilgen, I. Gosse, F. Diederich, *Top. Stereochem.*, submitted; F. Diederich, C. Thilgen, A. Herrmann, *Nachr. Chem. Tech. Lab.* **1996**, *44*, 9; A. Herrmann, M. W. Rüttimann, T. Giptner, C. Thilgen, F. Diederich, T. Mordasini, W. Thiel, *Helv. Chim. Acta* **1999**, *82*, 261, and refs. cit. therein.

Received February 4, 2000